JOURNAL OF
Applied Polymer
SCIENCE

Microstructural characterization of short glass fibre reinforced polyethersulfone composites: A positron lifetime study

L. M. Munirathnamma, H. B. Ravikumar
Department of Studies in Physics, Manasagangotri, University of Mysore, Mysuru 570006, India
Correspondence to: H. B. Ravikumar (E-mail: hbr@physics.uni-mysore.ac.in or ravi7010@rediffmail.com)

ABSTRACT: To explore the effect of short glass fiber reinforcement (SGFR) on the mechanical properties of polyethersulfone (PES), microstructural characterization has been performed by positron lifetime technique. The free volume distribution of SGFR-PES composites derived from CONTIN-PALS2 program exhibits the narrow full width at half maximum (FWHM) indicates the strong interaction between polymeric chains of PES matrix and SGF. The positron lifetime parameters of SGFR-PES composites are correlated with the mechanical properties viz., Tensile strength (TS), Young's modulus (YM) and elongation at break (EB). The decreased positron lifetime parameters, improved mechanical properties and reduced crystallinity of SGFR-PES composites are attributed to the improved chemical and physical interaction between the functional groups of both SGF and PES matrix. This is clearly evident from the FTIR (Fourier Transform Infrared Spectrometry) studies. The hydrodynamic interaction parameter (h) show negative values, suggest the improved interaction in SGFR-PES composites by the generation of excess friction at the interface. © 2016 Wiley Periodicals, Inc. J. Appl. Polym. Sci. **2016**, *133*, 43647.

KEYWORDS: biocompatibility; biomedical applications; composites; fibers; viscosity and viscoelasticity

Received 16 November 2015; accepted 14 March 2016
DOI: 10.1002/app.43647

INTRODUCTION

Now-a-days, fiber reinforced polymer (FRP) composites are widely used in the medical field, where the mechanical properties are a serious concern.[1] The conventional metallic/ceramic orthopedic implants are being replaced by FRP composites. The advantage of using FRP composites in load bearing orthopedic implants is mainly because of their lightweight, high strength and stiffness than the conventional metallic implants. This will reduce the "stress shielding' effect around the implants.[2] They exhibit high biocompatibility, non-corrosion and good bonding between the bone and implant.[3–5]

The most commonly used polymers for the orthopedic implants in the medical field are Polysulfone (PSU), Polybutylene terephthalate (PBT), Nylon, polymethyle methacrylate (PMMA), Polyetherimide (PEI), polyetheretherketone (PEEK), Polyethylene (PE) etc.[6] In the present study, due to its high strength, stiffness and good biocompatibility, Polyethersulfone (PES) was chosen as the polymer matrix. PES is an excellent heat resistant, transparent, non-crystalline engineering plastic containing ether groups and sulfone groups in its backbone chains.[7] PES resins are biocompatible, exhibit high dimensional stability and outstanding rigidity even at very high temperature. PES can be molded on conventional plastics processing equipment such as injection molding, extrusion, compression molding, solution casting and sintering. Because of its amorphous nature, PES has excellent dimensional stability and it can be easily processed with highly polar solvents.[8] Fiber reinforced PES composite materials are presently used to manufacture orthopedic devices to replace metal alloys.[9] The fiber reinforced PES composites are also used in automobile industry and aerospace materials as toughening and processing agents.[10]

In order to improve the mechanical properties of polymer composites, E-glass fibers are most commonly reinforced into the polymer matrix. The major problem associated with the untreated E-glass fibers is that they exhibit low interfacial adhesion between the fibers and thermoplastic matrix. This can be overcome by treating the surface of E-glass fiber with 3-Aminopropyltriethoxy (3-APE) silane coupling agent.[11–14] From the literature survey, it has been found that not much work has been done on short glass fiber reinforcement (SGFR) polymer composites and the effect of free volume on the mechanical properties of FRP composites are no where reported. Therefore, in the present study, authors made an attempt to correlate the free volume and mechanical properties of SGF reinforced PES for biomedical applications. To study the effect of fiber reinforcement on the microstructure of polymeric matrix, short glass fiber (SGF) of 10 to 40 wt % are reinforced into PES matrix. The microstructural characterization of SGFR-PES composites has been performed by one of the well-established, sophisticated tools viz., positron annihilation lifetime spectroscopy (PALS). In recent years, positron lifetime technique has emerged as a unique and potent probe for directly characterizing the free volume cavities and their concentration in the amorphous region of the polymers in terms of positron lifetime of the injected positrons.[15] The free volume holes provide pathways for thermal motion of the chain segments. The varieties of structural changes like first order phase transition, second order phase transitions like glass transition and relaxation processes in polymers and polymer composites are well described by considering the free volume as an internal material parameter.[16] The measured free volume parameters by PALS may not directly provide the changes occurring at the interface of the polymer-fiber composites. The friction developed between the interfaces of polymer/fiber is determined by the hydrodynamic interaction parameter (h) arises from the flow dynamics of polymer solutions.[17,18] To quantify the extent of interaction at the interface of SGFR-PES composites, hydrodynamic interaction parameter (h) has been evaluated. The mechanical properties viz., tensile strength (TS), and Young's modulus (YM) have been measured by Universal Testing Machine (UTM) as per ASTM-D 256 model.

THEORY

Hydrodynamic Interaction Parameter

The concept of hydrodynamic interactions in polymer solution was first introduced by Kirkwood and Riseman[17,18] in the year 1956. The hydrodynamic interaction is the mechanical interaction generated due to the excess friction between the constituents of the polymeric chains. The friction between the polymeric chains of the composites is not only due to the intermolecular interactions but also due to the intramolecular repulsion between them.[17,18] Polymer composites are the visco-elastic materials and exhibit time-dependent relaxations. The relaxation usually means to return from a perturbed system into equilibrium. The relaxation process can be characterized by a relaxation time (τ), which is related to the viscosity (η) and YM (σ) by the relation.[19]

$$\tau = \frac{\eta}{\sigma} \tag{1}$$

The hydrodynamic interaction parameter (h) is related to the relaxation time (τ) by the equation

$$\tau = \frac{\pi \eta_s r a^2}{2KT\left(1 - h\sqrt{\frac{6}{\pi}}\right)} \tag{2}$$

where "r" is the radius of the fibers, "a" is the length of the fibers, k is Boltzmann constant and "T" is the absolute temperature. From eqs. (1) and (2) hydrodynamic interaction parameter (h) can be written as

$$h = \frac{2kT - \sigma \pi r a^2}{2kT\sqrt{\frac{6}{\pi}}} \tag{3}$$

and it is more negative for composites having higher YM.[20,21]

EXPERIMENTAL

Materials

PES with a density of 1.31 g/cm^3 was procured from BASF Company (Ludwigshafen, Germany) under the trade name Ultrason. The chemical structure of PES is as shown in Figure 1. E-glass fibers with a mean diameter of 16 μm and the density of 2.60 g/cm^3 supplied by Nippon Electric glass, Taiwan were used as the reinforcement.

Silane Treatment

3-APE silane (0.6%) was mixed well with ethanol/water in the ratio 6:4 and kept for 1 h. The pH of the solution was maintained between 3.5 and 4 to complete the hydrolysis of silane by the addition of acetic acid. The E-glass fibers were dipped in the above solution for 1 h. In order to obtain the homogeneous dispersion of silane into the fiber surface, the mixture was continuously mixed for another 30 minutes. The length of the SGF after mixing is 3 mm and the thickness of the coating is about 0.14 mm. The treated E-glass fibers were then dried at 100 °C for about 5 h in an air circulating oven to evaporate ethanol completely. The interaction mechanism is as shown in Figure 2.

Preparation of Composites

PES and E-glass fiber were dried around 150 °C for 6 h and at 120 °C for 2 h respectively. PES granules and 3 mm SGF of various loading (10, 20, 30 and 40 wt % were mixed in a Haake co rotating twin screw extruder (diameter = 40 mm, L/D = 16) operating at a barrel temperature profile ranging from 343 °C to 377 °C at the feed rate of 1 kg/h and a screw speed of 230 rpm. The extruded composites were subsequently pelletized by a granulator. The reinforced granules were then molded on an injection molding machine with an injection pressure from 69 to 103 MPa. The mold temperature was held at 135 °C to 177 °C respectively. After molding, the specimens were allowed to cool at room temperature.

Measurements

Positron Annihilation Lifetime Measurements. Positron annihilation lifetime spectra of PES matrix and SGF reinforced Polyethersulfone (SGFR-PES) composites for different fiber concentration were recorded using a standard fast-fast coincidence system with conically shaped BaF_2 scintillators coupled to photomultiplier tubes of type XP2020/Q with quartz window as detectors.[15] The coincidence lifetime spectrometer had a resolution of 230 ps. The two identical pieces of the samples were placed on either sides of a 15 μCi - ^{22}Na positron source deposited on a pure Kapton foil of 0.0127 mm thickness. This sample-source sandwich was placed between the two detectors to acquire lifetime spectrum. All lifetime measurements were performed at room temperature and two to three positron lifetime spectra with more than a million counts under each spectrum were recorded in a time of 2–4 hrs.[15] Consistently reproducible spectra were analyzed into three lifetime components with the help of the computer program PATFIT-88[22] and

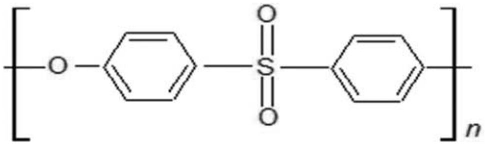

Figure 1. The chemical structure of PES.

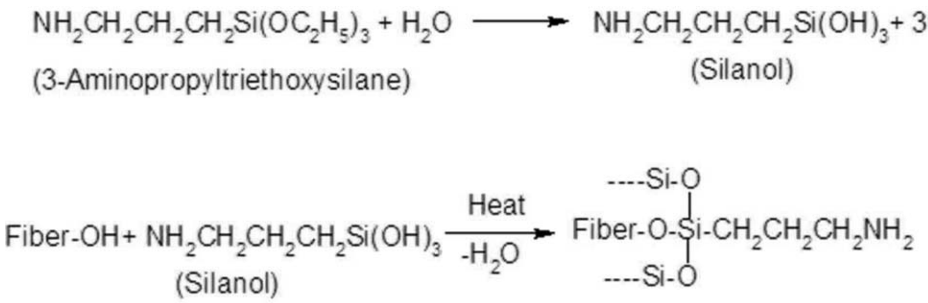

Figure 2. Mechanism of silane treatment of E-glass fibers.

CONTIN-PALS2 with proper source and background corrections. Source correction term and resolution function were estimated from the lifetime of well annealed aluminium using the program RESOLUTION.[22] The three Gaussian resolution functions were used in the present analysis of positron lifetime spectra of as received PES and SGFR-PES for different fiber concentration. The o-Ps lifetime τ_3 is related to the free volume hole size by a simple relation given by Nakanishi et al.,[23] which was developed on the basis of theoretical models originally proposed by Tao[24] for molecular liquids and later by Eldrup et al.[25] In this model, Positronium is assumed to be localized in a spherical potential well having an infinite potential barrier of radius R_o with an electron layer in the region $R < r < R_o$. The relation between "τ_3" and the radius R of the free volume hole or cavity is,

$$\lambda=\frac{1}{\tau_3}=2P=2\left[1-\left(\frac{R}{R_o}\right)+\left(\frac{1}{2\pi}\right)\sin\left(\frac{2\pi R}{R_o}\right)\right]\text{ns}^{-1} \quad (4)$$

where $R_o = R+\Delta R$ and ΔR is an adjustable parameter. By fitting eq. (4) with τ_3 values for known hole sizes in porous materials like zeolites, a value of $\Delta R = 1.657$ Å was obtained. With this value of ΔR, the free volume radius R has been calculated from eq. (4) and the average size of the free volume holes (V_f) is evaluated as

$$V_f=\frac{4}{3}\pi R^3 \quad (5)$$

The fractional free volume or the free volume content (F_v) can then be estimated as

$$F_v=CV_f I_3 \quad (6)$$

where C is structural constant, whose value is taken as 0.0018 Å^3, V_f is the free volume hole size, and I_3 is the o-Ps intensity.

In order to analyse the acquired positron lifetime spectra computer program CONTIN-PALS2 is used. CONTIN-PALS2 program is based on the inverse Laplace transformation technique and this generates the distribution of annihilation rate probabilities (probability density function [PDF]) of free volume cavity radius and size. For the analysis of annihilation rate probability solutions, 90 grids in the annihilation rates from 0.35 to 9 ns^{-1} are selected and the appropriate "α" regularizer was constrained to 2.5×10^{-3}. The moment of order (-1) displayed in the output was used to evaluate the mean o-Ps lifetime and intensities. The PATFIT analysis is also made to check the correctness of the CONTIN results. The results of three annihilation rate distributions obtained from CONTIN-PALS2 corresponding to the three lifetime components (τ_1, τ_2 and τ_3) are agree well with the values obtained by PATFIT program. These results are shown in Table I.[26,27]

The CONTIN analysis provides the annihilation rate PDF $\alpha(\lambda)$ to the corresponding radius PDF for the free-volume regions in which o-Ps annihilates is obtained from eq. (7), which relates the annihilation rate λ with free volume radius R. Then the fraction of positrons annihilating in cavities with radii between R and $R + \Delta R$ is $f(R)\ \Delta R$. The free volume radius PDF: $f(R)$ is given by Refs. 26 and 27.

$$f(R)=2(\Delta R)\left\{\cos\left[\frac{2\pi R}{(R+\Delta R)}\right]-1\right\}\frac{\alpha(\lambda)}{(R+\Delta R)^2} \quad (7)$$

Where ΔR has the same meaning as defined earlier.

Then the fraction of positrons annihilating in cavities with volumes between V and $V+\ dV$ is given by $g(V)\ dV$. The free volume PDF assuming a spherical cavity is

$$g(V)=\frac{f(R)}{4\pi R^2} \quad (8)$$

Mechanical Property Measurements. Mechanical properties namely TS, tensile modulus and elongation at break (EB) for

Table I. Comparison of Free Volume Data Derived from the Two Programs PATFIT and CONTIN-PALS2

	PATFIT-88 Analysis			CONTIN- PALS2 Analysis			
Sample	τ_3 (ns) ± 0.013	I_3 (%) ± 0.22	V_f (Å^3) ± 0.9	τ_3 (ns) ± 0.018	I_3 (%) ± 0.24	V_f (Å^3) ± 0.3	FWHM (Å)
Pure-PES	1.832	15.67	82.17	1.825	15.60	81.53	2.654
PES + 10 wt % SGF	1.821	16.75	81.17	1.820	16.78	81.08	2.650
PES + 20 wt % SGF	1.818	17.21	80.89	1.814	17.28	80.53	2.645
PES + 30 wt % SGF	1.782	15.80	77.68	1.787	15.78	77.51	2.630
PES + 40 wt % SGF	1.779	14.05	77.42	1.775	14.11	77.33	2.618

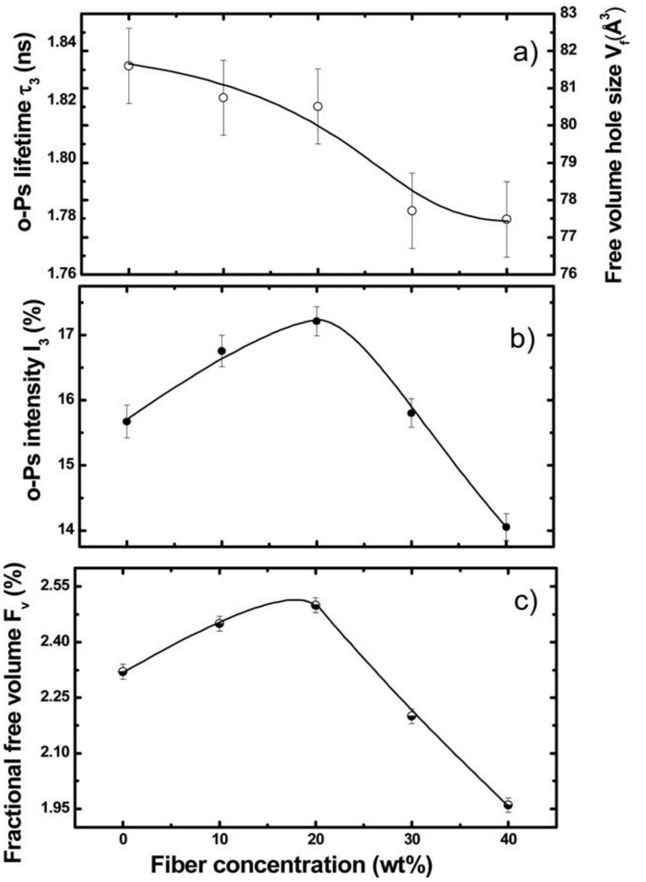

Figure 3. Plot of free volume parameters (a) o-Ps lifetime (τ_3) and free volume hole size (V_f) (b) o-Ps intensity (I_3) and (c) fractional free volume (F_V) as a function of fiber concentration.

different fiber concentration of the composites were measured according to ASTM D 638 standard using Universal Testing Machine (UTM), model 4302 H50 KM, 50KN, Hounsfield, UK. Three samples were tested for each concentration and the average value has been reported.

X-ray Diffraction Studies. X-ray diffraction patterns of the samples were recorded using Rigaku Mini Flex 11 diffractometer with Ni filtered Cukα radiation of wavelength 1.5406 Å with graphite monochromator. X-ray difftraction spectra of as received PES matrix and SGF reinforced polyethersulfone (SGFR-PES) composites for different fiber concentration were taken in a glass sample holder. The X-ray scans were recorded in the 2θ range from 6°–60° with a scan speed of 5°/min in steps of 0.02°. The working voltage and current were 30 kV and 15 mA respectively.

FTIR Studies. FTIR experiment was carried out using a Perkin Elmer Spectrum Version (model spectrum 2 series, NIOS2 Main software, USA) fitted with a Personal Computer (PC) for data processing. It is a well-established technique for investigation of functional groups in the fiber and polymer matrix. The functional groups can either be organic or inorganic. FTIR spectra of as received PES matrix and SGF reinforced polyethersulfone (SGFR-PES) composites for different concentration were run at ambient temperature using KBr disk method at the wave number range of 4000–500 cm^{-1}.

Results and Discussions

Positron Lifetime Results. Positron lifetime studies of FRP composites reveal that the free volume properties of polymer composites are strongly affected by the amount and type of fiber used for reinforcement.[28,29] As we are interested on the free volume hole size and their concentration of fiber reinforced PES composites, only the third lifetime component viz., o-Ps lifetime (τ_3) and o-Ps intensity (I_3) derived from PATFIT program are reported here. Figure 3 shows the plots of o-Ps lifetime (τ_3) and free volume size (V_f), o-Ps intensity (I_3) and fractional free volume (F_v) as a function of fiber concentration respectively. To account for the fraction of positrons annihilating in glass fibers, positron lifetime measurements have been performed on the glass fibers alone, which yielded $\tau_3 = 1.03$ ns and $I_3 = 7.66\%$. From the Figure 3(a) it is observed that the values of o-Ps lifetime (τ_3) and its intensity (I_3) of PES matrix are 1.832 ns and 15.67% respectively. The o-Ps lifetime (τ_3) decreases gradually as a function of fiber concentration and about 53 ps (picoseconds) reduction occurs from 1.832 ns to 1.779 ns (nanoseconds) at 40 wt % of fiber. This corresponds to the reduction of free volume hole size (V_f) from 82.17 Å^3 to 77.42 Å^3 at 40 wt % of SGF. This reduction in free volume hole size in SGFR-PES composites can be explained as follows.

The E-glass fibers are treated with silane coupling agent will have polysilaxone networks and these networks consist of large number of active functional groups. They can easily undergo chemical and physical interactions with side chains of PES matrix by hydrogen or covalent bonding and van der Waals type of attractive forces.[11,14] Therefore, the decreased o-Ps lifetime from 1.832 ns to 1.779 ns at 40 wt % SGF reinforced PES matrix is attributed to the improved adhesion between SGF and PES matrix due to the induced chemical and physical interactions.

The variation of o-Ps intensity (I_3) as a function of SGF concentration is as shown in Figure 3(b). From the figure it is observed that about 1.54% increase of o-Ps intensity (I_3) at 20 wt % of SGF and the reduction of 3.16% from 20 wt % to 40 wt %. The intensity of o-Ps annihilation (I_3) correlates with the amount of free volume or the number of voids in the sample. The increase of o-Ps intensity (I_3) at 20 wt % of SGFR-PES composites is attributed to the formation of additional voids at the interface. The decrease in o-Ps intensity (I_3) at 40 wt % of SGF is due to the reduction in number density of o-Ps annihilation sites. This is due to the restriction on the segmental motion of the polymeric chains of PES caused by the strong interaction between the PES matrix and SGFs.[30,31] The fractional free volume (F_v) is derived from the product of free volume hole size (V_f) and o-Ps intensity (I_3) would rather represents the overall changes in free volume of the system.[32] Figure 3(c) shows the variation of fractional free volume (F_v) calculated according to the eq. (7) as a function of SGF wt %. The fractional free volume (F_v) increases up to 20 wt % of SGF is due to the loose packing of polymeric chains in SGFR-PES composite. The decreased F_v at 40 wt % of SGF indicates the

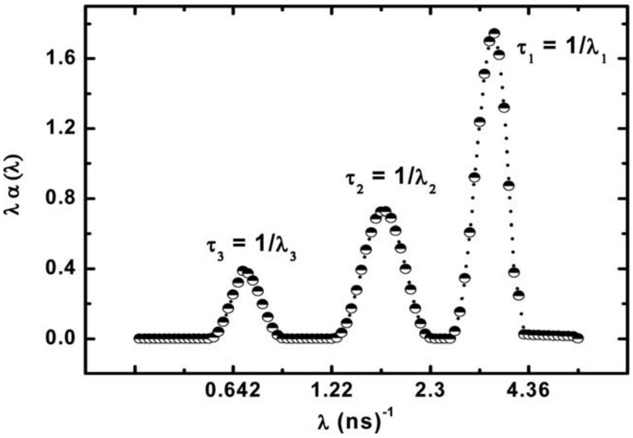

Figure 4. Positron annihilation rate PDF for polymer composites. Peak τ_3 represents *ortho*-Positronium (o-Ps) annihilation rate PDF.

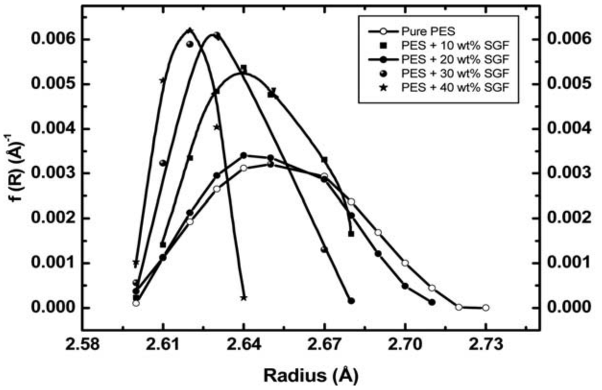

Figure 5. Free volume hole radius PDF [f(R)] and Free volume hole size PDF [$g(V)$] for (a) Pure PES matrix (b) PES + 10 wt % SGF (c) PES + 20 wt % SGF (d) PES + 30 wt % SGF (e) PES + 40 wt % SGF.

improved molecular packing between SGF and PES matrix due to the improved physical and chemical interaction.[33]

Free Volume Distribution (CONTIN-PALS2) Results. The analysis of size distribution of free volume cavities was carried out to estimate the most probable size of free volume cavities in the SGFR-PES composites for different fiber content. The distribution of lifetimes in pure PES and composites are derived from CONTIN-PALS2 is as shown in Figure 4. The first peak from the left corresponds to o-Ps lifetime distribution.[26,27] The free volume radius distribution f(R) as a function of free volume radius (R) and hole size g (V) as a function of free volume size (V_f) in SGFR-PES composites is as shown in Figure 5. The free volume radius/size distribution of each sample is distinct with regard to its spread and height and in few cases in shape as well. SGFR-PES composites show variety in their free volume hole radius/size distribution and full width at half maximum (FWHM).

From the Figure 5 it is observed that the free volume size distributions obtained from SGFR-PES composites appear more or less Gaussian. PES exhibits broad free volume size distribution and its FWHM is about 2.654 Å. SGFR-PES composites with 10 to 40 wt % of SGF show relatively narrow distributions. Generally, broader distribution in polymer composites is attributed to the formation of interfacial region between the matrix and the SGF and hence the formation of bigger free volumes.[34] The narrower distribution obtained in SGFR-PES composites with 10 - 40 wt % SGF is due to the close packing resulted by the strong interaction between the constituents.[34] The specific interaction between the constituents is explained with the help of FTIR spectra. The free volume data derived from the two programs PATFIT and CONTIN-PALS2 results are shown in Table I.

X-ray Diffraction Results. Figure 6 shows the XRD spectra of pure PES and SGFR-PES composites with 10 to 40 wt % SGF reinforced into PES matrix. X-ray diffraction pattern of FRP composites contain both sharp as well as diffused peaks. In which, sharp peaks correspond to crystalline domain and diffused peaks for amorphous regions of polymer samples. XRD spectra of pure PES and SGFR-PES composites of different concentrations show a sharp crystalline peak at $2\theta = 19°$. The intensity of crystalline peak of SGFR-PES composites decreases as a function of SGF wt % indicates the increased amorphousity of SGFR-PES composites. When silane coupling agent reacts with hydroxyl group of E-glass fiber, alkoxy silane undergoes hydrolysis and form polysiloxane structure by hydrogen bond formation. The large coupling molecules will damage the packing of the glass fiber chains and causes disturbance in the crystalline pattern of the main polymeric backbone[14,35] and hence increases the amorphousity of the composites.

Correlation between Free Volume Parameters and Mechanical Properties Results. The mechanical properties are considered as the most important of all the physical properties for structural applications. The free volume cavities and their concentration have been used in understanding the visco-elastic properties of the many polymeric systems.[36] In the present study, mechanical properties viz., TS, YM, and EB of SGFR-PES composites for different fiber concentration are measured at ambient conditions and correlated with free volume parameters. This property depends on the chain morphology of the system i.e. the ease with which the chains can slide past each other under the influence of any external force. The variation of free volume size (V_f), TS, YM, and Elongation at break (EB) as a function of

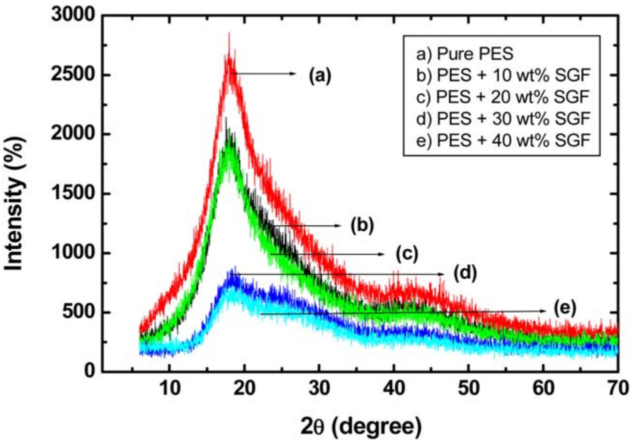

Figure 6. XRD spectra of pure PES and SGFR-PES composites at different fiber concentration. [Color figure can be viewed in the online issue, which is available at wileyonlinelibrary.com.]

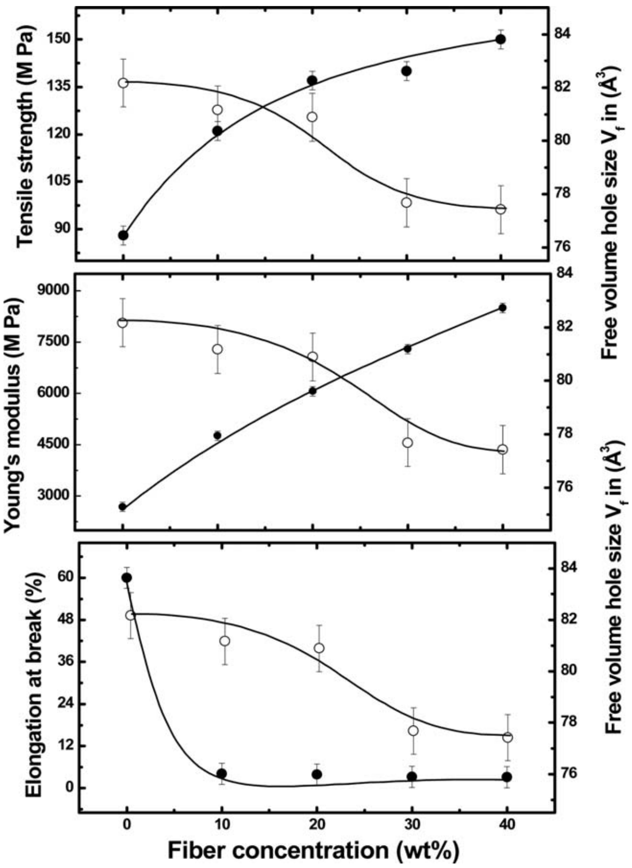

Figure 7. Plot of Free volume hole size and Mechanical Parameters against fiber concentration for SGFR-PES composites.

fiber concentration are shown in Figure 7. At 40 wt % SGFR-PES composite, both TS and YM showed greatest improvement in their values and the EB of 40 wt % SGFR-PES composite shows a minimum value. On the other hand the reduction of about 4.75 $Å^3$ free volume hole size is evident at 40 wt % of SGFR. The reduction of free volume hole size (V_f), increased TS and YM can be correlated as follow. The addition of silane treated glass fibers into the polymer matrix initiates the chemical and physical interaction[36] in SGFR-PES composites. The close packing resulted between the fiber and matrix due to the strong interaction provides less space for the chain movement and hence reduces the free volume hole size. This would be the one of the reasons for increased TS and YM of 40 wt % SGFR-PES composite. The decreased EB is due to the reduced ductility of SGFR-PES composite due to the incorporation of SGFs.[36]

Hydrodynamic Interaction Parameter Results. The FRP composites have a distinctive combination of physical, mechanical, thermal and rheological properties. The strength of the adhesion between the polymer-fiber composite at the interface can be represented by the hydrodynamic interaction parameter (h). The hydrodynamic interaction refers to the excess friction generated at the interface of polymer and reinforced fiber.[17,18] In FRP composites, there exists an attractive interaction between the polymeric chains of the constituents; therefore one would expect high friction between them. In such circumstances the hydrodynamic interaction parameter (h) attains large negative values. Suppose, if the friction is less at the interface due to the lack of interaction between the polymeric chains of the constituents, each polymer forms its own domain in the system and results to the reduced contact between the polymer chains. For such system hydrodynamic interaction parameter (h) becomes positive.[17,18] In SGFR-PES composites, the silane treated glass fibers are randomly distributed on PES matrix. The sites of the interaction between the constituent polymeric chains are maximum, thus when a chain attempts to move, it is pulled by several other chains with which it has segmental level interaction. This provides more friction at the interface and improves the adhesion between the constituents of SGFR-PES composites; this is determined by hydrodynamic interaction parameter (h).[17,18] Figure 8 shows the plot of hydrodynamic interaction parameter (h) evaluated by eq. (3) as a function of fiber concentration. The "h" parameter for pure PES is about (-1.82×10^{18}) and this value decreases as the concentration of glass fiber in the composite increases and it becomes more negative for 40 wt % of SGFR-PES composite. This indicates that the hydrodynamic interaction at 40 wt % SGFR-PES composite is very high due to the excess friction developed at the interface of SGFR-PES composite. This excess friction is due to the intramolecular repulsion between the polymeric chains of PES.[17,18] The improved mechanical strength and decreased hydrodynamic interaction parameter at 40 wt % of SGFR-PES composite can be attributed to the increased interfacial strength between SGF and PES matrix.[37]

FTIR Results. Fourier transform infrared spectrometry (FTIR) is used to study the chemical interaction between silane treated E-glass fiber and PES matrix. The FTIR spectrum of silane treated E-glass fiber measured in transmittance mode is as shown in Figure 9(a). This shows the prominent transmittance peak at 920 cm^{-1} corresponding to the –Si–C–asymmetric stretching.[38] The bands at 1,222 cm^{-1} is due to the asymmetric stretching of –Si–O–Si– and/or to the –Si–O–C– bonds.[39] The band at 1800 cm^{-1} and 1401 cm^{-1} correspond to the twisting vibration of NH_2 group hydrogen bonded to the hydroxyl group of both silane and the fiber surface, indicating the complete adsorption of silane on to the fiber surface. This confirms the grafting of silane on to the fiber surface after the silane treatment.

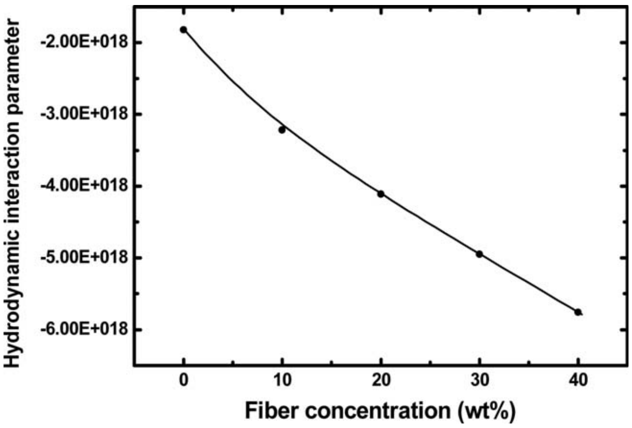

Figure 8. Hydrodynamic interaction parameter for SGFR-PES composites as a function of SGF concentration.

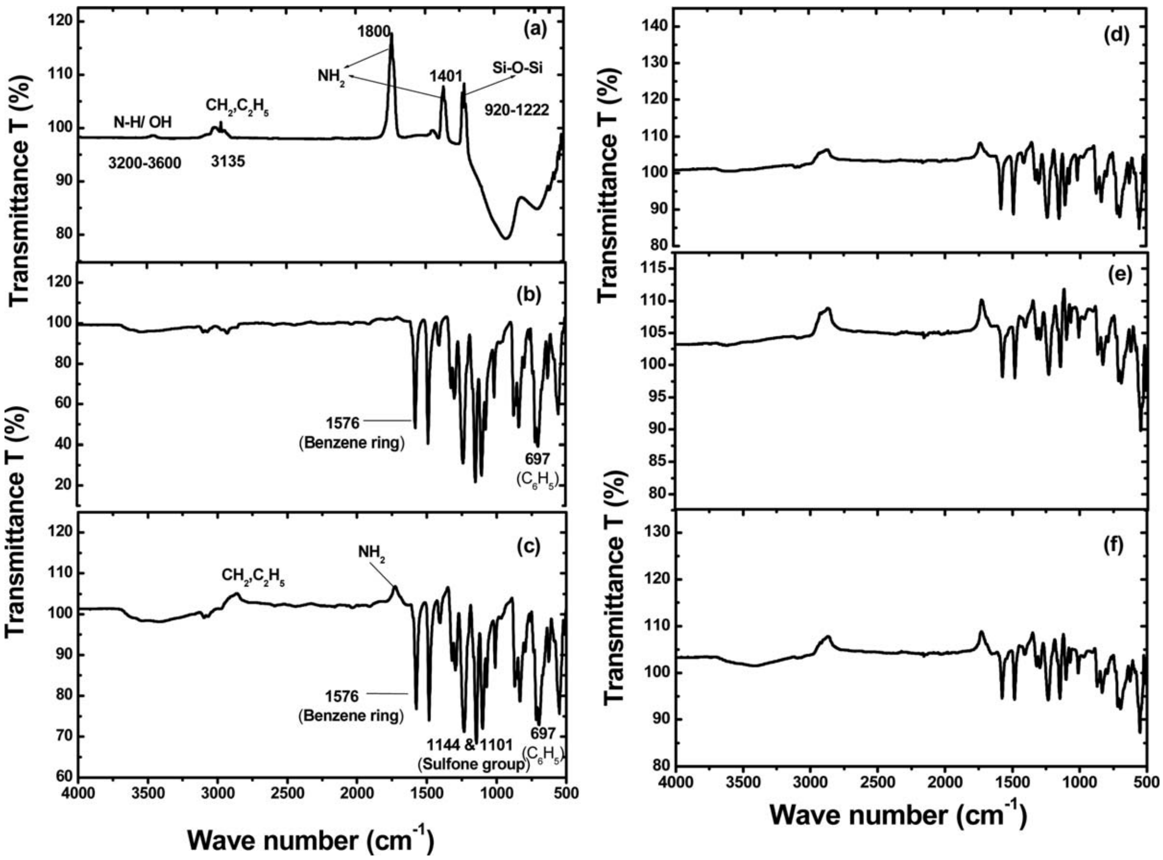

Figure 9. FTIR spectra of (a) silane treated E-glass fiber (b) pure-PES matrix (c) PES + 10 wt % SGF (d) PES + 20 wt % SGF (e) PES + 30 wt % SGF (f) PES + 40 wt % SGF.

This is as shown in Figure 2. Apart from this, silane coupling agent also introduces an organosiloxy group to the fiber surface.[38]

FTIR spectra of silane treated SGF reinforced pure PES matrix, 10%, 20%, 30%, and 40 wt % SGFR-PES composites measured in transmittance mode are shown in Figure 9(b–f) respectively. The PES structure includes a benzene ring, an ether bond and a sulfone (SO_2) group. The FTIR spectrum of pure PES matrix shows the continuous transmittance peak at 3068 cm^{-1} corresponding to the C—H stretching peak of benzene ring. The peaks at 1576 cm^{-1} and 1405 cm^{-1} were attributed to C—C and C=C stretching vibrations in the Benzene ring. The C—O—C stretching peaks were located at 1319 cm^{-1} and 1233 cm^{-1}. The peaks at 1144 and 1296 cm^{-1} (strong) indicate the presence of sulfone (SO_2) groups.[40]

The collection of bands around 2961–2875 cm^{-1} are the stretching of C—H, CH_2, C_2H_5 and phenyl ring both in aromatic and aliphatic compounds.[39] The band at 1100 cm^{-1} is assigned to stretching of C–O and Si–O indicates the presence of silicon oxide compounds attached to PES matrix.[39] The band at 1484 cm^{-1}, 1071 and 757 cm^{-1} corresponds to the bending vibrations of methylene and phenolic C—H bonds respectively.[40,41] The broad band between 3600-3200 cm^{-1} indicates the presence of hydroxyl groups and a peak at 697 cm^{-1} is characteristic of —C_6H_5 (phenyl groups).[42–47] Figure 9(c–f) suggest the formation of hydrogen bonding between amine groups attached to trimetylene group of silane treated E-glass fiber and sulfone (SO_2) group of PES matrix. This chemical interaction between E-glass fiber and sulfone (SO_2) group of PES matrix is shown in Figure 10. Although, hydrogen bonding is more likely to provide the strong interfacial interaction between the fiber and the polymer matrix,[41] there may be van der Waals type of attractive forces and hydrodynamic interaction established between polymeric chains of PES matrix and the long hydrophobic chain of polymerized silane.[11,14] This would be the one of the reasons for the decreased free volume hole size (V_f) from 82.17 $\AA^3$ to 77.42 $\AA^3$ and improved mechanical strength of 40 wt % SGFR-PES composite. The reduction in peak intensity at 1576 cm^{-1}, 1405 cm^{-1} and 697 cm^{-1} in the FTIR spectrum indicates increased IR absorption due to the induced molecular packing in the SGFR-PES composites.[15]

Conclusions

The decreased value of positron lifetime parameters viz., o-Ps lifetime (τ_3), free volume hole size (V_f) and improved TS, YM, and reduced EB upon SGFR indicate the good adhesion between the fiber and PES polymer matrix. The decreased o-Ps intensity at the higher concentration of SGF suggests the reduction in number density of o-Ps annihilation sites due to the restriction on the segmental motion of the polymeric chains of PES caused by the strong interaction between the PES matrix and SGFs. The free volume distribution derived from CONTIN-PALS2 program exhibit relatively narrow FWHM for 40 wt % of SGFR-PES composites indicates the strong interaction

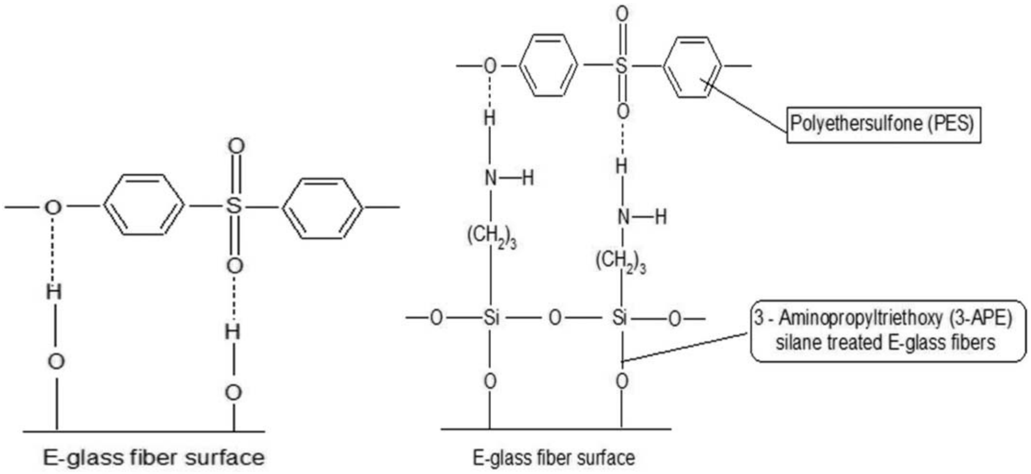

Figure 10. Schematic representation of interfacial interaction for Non-treated E-glass fiber and silane treated E-glass fiber with PES matrix.

between PES matrix and SGFs. The reduced intensity of crystalline peak upon fiber loading suggests the grafting of silane on to the glass fiber surface. The FTIR result confirms the induced chemical interaction by the hydrogen bonding between the amine groups of silane treated E-glass fiber and sulfone group of PES matrix. Along with the chemical interaction the contribution of hydrodynamic interaction is also predominant for the improved interfacial adhesion between the polymeric chains of PES matrix and the SGFs. SGFR-PES composite with 40 wt % of SGF can be used as the replacement of metal alloys for load bearing orthopedic applications. Further investigations are necessary for the improvement of mechanical strength of SGFR-PES composite for specific applications.

ACKNOWLEDGMENTS

One of the authors (L.M.M.) is thankful to UGC, India for providing Junior Research Fellowship (JRF) to carry out this research work. Authors are also grateful to S. Srinivas, Brakes India Limited, Nanjangud; Mysore for providing the SGF reinforced Polyethersulfone (SGFR-PES) composites for this study.

REFERENCES

1. Fujihara, K.; Huang, Z. M.; Ramakrishna, S.; Satknanantham, K.; Hamada, H. *Biomaterials* **2004**, *25*, 3877.
2. Mattila, R. H.; Laurila, P.; Rekola, J.; Gunn, J.; Vallittu, P. K. *Acta Biomater.* **2009**, *5*, 1639.
3. Sabir, M. I.; Li, X. *J. Mater. Sci.* **2009**, *44*, 5713.
4. Zairi, F.; Abdelaziz, M. N. *Int. J. Sol. Struct.* **2008**, *45*, 5220.
5. Ravishankar, R.; Chandrashekara, K. *Int. J. Mech. Eng. Technol.* **2013**, *4*, 197.
6. Wu, G. M.; Schultz, J. M. *J. Polym. Compos.* **2000**, *21*, 223.
7. Fan-Long, J.; Seul-Yi, L.; Soo-Jin, P. *Car. Lett.* **2013**, *14*, 76.
8. Black, J.; Hastings, G. Handbook of Biomaterial properties: Chapman & Hall: London: **1998**.
9. Ainsworth, R. D.; Thirumalai, N. C. D.; Steven, T. C. L. U.S. Patent 4,892,552, **1990**.
10. Yuan, H.; Zhang, S.; Lu, C.; He, S.; An, F. *Appl. Surf. Sci.* **2013**, *279*, 279.
11. Jacob, M.; Thomas, S. *J. Appl. Polym. Sci.* **2004**, *93*, 2305.
12. Suardana, N. P. G.; Piao, Y.; Lim, J. K. *Mater. Phys. Mech.* **2011**, *11*, 1.
13. Radojevic, V.; Stojanovic, D. Influence of Silane Coupling Agents on the Mechanical Properties of Recycled Glass-Fibre Reinforced Composites; Workshop, University of Belgrade, Serbia.
14. Sreekumar, P. A.; Thomas, S. P.; Saiter, J. M.; Joseph, K.; Unnikrishnan, G.; Thomas, S. *Compos. Part A* **2009**, *40*, 1777.
15. Aneesh Kumar, K. V.; Ravikumar, H. B.; Ranganathaiah, C. *J. Appl. Polym. Sci.* **2013**, *130*, 793.
16. Ravikumar, H. B.; Ranganathaiah, C.; Kumaraswamy, G. N.; Thomas, S. *J. Polym.* **2005**, *46*, 2372.
17. Naito, K.; Johnson, G. E.; Allara, D. L.; Kwei, T. K. *Macromolecules* **1979**, *11*, 1260.
18. Nishimoto, N.; Keskkula, H.; Paul, D. R. *J. Polym.* **1989**, *30*, 1279.
19. David, R. Engineering Viscosity Creep and Relaxation of Nonlinear Viscoelastic Materials; Dover Publications: New York, **1989**.
20. Bird, R. B.; Curtiss, C. F.; Armstrong, R. C.; Hassager, O. Dynamics of Polymeric Liquids; Wiley & Sons Inc, **1987**.
21. Macosko, C. W. Rheology: Principles, Measurements, and Applications; Wiley-VCH: New York, **1994**.
22. Kierkegaard, P.; Pedersen, N. J.; and Eldrup, M. Riso National Laboratory Reports; RISO-M-274, Denmark, **1989**.
23. Nakanishi, H.; Wang, S. J.; and Jean, Y. C. Positron Annihilation in Fluids; Sharma, Ed., World Scientific: Singapore, **1988**.
24. Tao, S. J. *J. Chem. Phys.* **1972**, *56*, 5499.
25. Eldrup, M.; Lightbody, D.; Sherwood, J. N. *Chem. Phys.* **1981**, *63*, 51.
26. Gregory, R. B. CONTIN (PALS2) User's Manual: A Modification of CONTIN (Version 2) for the Determination of

Positron annihilation Lifetime Distributions; Kent State University: Kent, Ohio, **1995**.

27. Provencher, S. W. CONTIN Users Manual Part 1: A Portable Fortran IV Program for the Regularized Solution of Linear Algebraic and Linear Integral Equations of the First Kind, With Options for Linear Equality and Inequality Constrains, Technical Report, EMBL-DA07, MaxPlanck-Institut Für Biophysikalishe Chemie: Göttingen, Germany, **1984**.
28. Emad, H. A. *Am. J. Appl. Sci.* **2011**, *8*, 147.
29. Awad, S.; Chen, H. G. *Macromolecules* **2011**, *44*, 29.
30. Deepa Urs, M. V.; Ranganathaiah, C.; Ramani, R.; Lal, B.; Alam, S. *J. Appl. Polym. Sci* **2006**, *102*, 2784.
31. Hammannavar, P. B.; Hundekar, M. Y.; Ravindrachary, C. B.; ; Blaise Lobo, V. *Int. J. ChemTech Res.* **2014**, *6*, 1867.
32. Paranhos, C. M.; Soares, B. G. *Eur. Polym. J.* **2007**, *43*, 4882.
33. Kumaraswamy, G. N.; Ranganathaiah, C.; Deepa Urs, M. V.; Ravikumar, H. B. *Eur. Polym. J.* **2006**, *42*, 2655.
34. Ramya, P.; Ranganathaiah, C. *J. Appl. Polym. Sci.* **2013**, DOI: 10.1002/app.37872.
35. Singha, A. S.; Rana, A. K. *J. Appl. Polym. Sci.* **2012**, *124*, 2473.
36. Altaweel, A. M.; Ranganathaih, C.; Ravikumar, H. B. *J. Polym.* **2005**, *46*, 2372.
37. Ramya, P. "Studies on the Interface Chacteristics of Immiscible Polymer Blends by Positron Lifetime Spectroscopy," PhD Thesis, University of Mysore, Mysuru, **2013**.
38. Gupta, A. K.; Biswal, M.; Mohanty, S.; Nayak, S. K. *Adv. Mech. Eng.* **2012**, *4*, 418031.
39. Joseph, S.; Sreekumar, P. A.; Kenny, J. M.; Puglia, D.; Thomas, S.; Joseph, K. *Polym. Eng. Sci.* **2010**, *50*, 1853.
40. Petersen, H. N.; Kusano, Y. *34th Riso. Int. Sym. Mater. Sci.* **2014**, *34*, 333.
41. Piccinini, P.; Senaldi, C.; Alberto Lopes, J. F. "Fibre Labelling Polytrimethylene Yerephthalate–PTT"-DuPont, JRC Scientific and Policy reports, European Commission, **2014**.
42. Yamashita, T.; Tomitaka, H.; Kudo, T.; Horie, K.; Mita, I. *Polym. Degrad. Stabil.* **1993**, *39*, 47.
43. Rivaton, A.; Gardette, J. L. *Polym. Degrad. Stabil.* **1999**, *99*, 385.
44. Gesner, B. D.; Kelleher, P. G. *J. Appl. Polym. Sci.* **1968**, *12*, 1199.
45. Monney, L.; Dubois, C.; Chambaudet, A. *Polym. Degrad. Stabil.* **1998**, *56*, 357.
46. Wavhal, D. S.; Fisher, E. R. *Desalination* **2004**, *172*, 189.
47. Linares, A.; Acosta, J. L. *J. Appl. Polym. Sci.* **2004**, *92*, 3030.

SGML and CITI Use Only
DO NOT PRINT